Recovery of Precious Metals (Au, Ag, Pt, and Pd) from Urban Mining Through Copper Smelting

MIN CHEN, KATRI AVARMAA, LASSI KLEMETTINEN, HUGH O'BRIEN, DMITRY SUKHOMLINOV, JUNJIE SHI, PEKKA TASKINEN, and ARI JOKILAAKSO

With the aim of investigating deportments of precious metals in pyrometallurgical processing of waste electrical and electronic equipment, the distributions of selected precious metals (gold, silver, platinum, and palladium) between copper matte and three different silica-saturated slags (pure FeO_x-SiO_2, FeO_x-SiO_2-Al_2O_3, and FeO_x-SiO_2-Al_2O_3-CaO slag) were investigated at 1300 °C in controlled flowing CO-CO_2-SO_2-Ar gas atmosphere by a high-temperature isothermal equilibration technique. The phase compositions were analyzed by Electron Probe X-ray Microanalysis and Laser Ablation-High Resolution Inductively Coupled Plasma-Mass Spectrometry. It was shown that the distribution coefficients of gold, platinum, and palladium between matte and slag ($L^{m/s}(Me) = [Me]_{in\ matte}/(Me)_{in\ slag}$) were very high and increased with increasing matte grade. The distributions to the matte phase were increased by adding basic oxides alumina and lime into the acidic silicate slags. The experimentally measured distribution coefficients $L^{m/s}(Me)$ followed the order of platinum > palladium > gold > silver. The present experimental results can be used for upgrading thermodynamic databases for the complex recycling processes through nonferrous smelting.

https://doi.org/10.1007/s11663-020-01861-5

I. INTRODUCTION

COPPER has been playing an essential role in our daily lives for thousands of years. It is mainly extracted from sulfide ores through pyrometallurgical processes.[1,2] It has been reported that about 600 million tons of copper were produced during the past two hundred years, of which around 20 pct was produced by Outotec flash smelting technology.[3] However, because of continuous depletion of ore-based copper mineral resources, as well as tighter environmental regulations and stronger demands for actions towards circular economy,[4] secondary copper resources such as industrial copper scrap and waste electrical and electronic equipment (WEEE) are increasingly being regarded as important copper resources.

WEEE is currently one of the fastest-growing waste streams[5–8] and its utilization as a secondary raw material is called urban mining. It is a valuable raw material as it is higher than the natural ores in precious metals (PMs) and platinum group metals (PGMs),[8,9] used in the electronics industry as a hybrid paste in the printed circuit board for improving electrical conductivity of joints.[10,11] Moreover, the environmental impact, as well as the associated production cost of precious metals from secondary sources, is much lower than those in the primary production from original ores.[9]

Currently, WEEE is mainly processed by incineration followed by a hydrometallurgical or pyrometallurgical treatment.[8] However, toxic gas emissions, such as dioxins and furans,[12,13] or waste water are produced during the incineration and hydrometallurgical leaching, which is harmful to the environment and human body health. A typical industrial practice for recycling WEEE is through primary and secondary copper smelting.[14–17] The key advantages of its pyrometallurgical processing are the availability to large-scale production, utilization of the heat generated by burning of plastic, and easy control of the dust and gas emissions without additional investment in an existing plant.[18] In industrial practices,

MIN CHEN, KATRI AVARMAA, LASSI KLEMETTINEN, JUNJIE SHI1, PEKKA TASKINEN, and ARI JOKILAAKSO, are with the Department of Chemical and Metallurgical Engineering, School of Chemical Engineering, Aalto University, Kemistintie 1F, P.O. Box 16100, 00076 Aalto, Finland. Contact e-mail: pekka.taskinen@aalto.fi HUGH O'BRIEN is with the Geological Survey of Finland, Vuorimiehentie 2, 02150 Espoo, Finland. DMITRY SUKHOMLINOV is with the Department of Materials Science and Engineering, Norwegian University of Science and Technology, 7491, Trondheim, Norway.

Manuscript submitted January 16, 2020.
Article published online May 19, 2020.

the delivered energy from the WEEE plastics has been estimated to be > 33000 MJ/t, and the concentrations of chlorinated dioxins/furans post the off-gas cleaning are below the legal emission limit of 0.1 ngTEQ/Nm^3,[14] indicating a low impact to the environment.

WEEE has a complex composition, including a variety of base metals (such as Cu, Al, Pb, Sn, Ni, Zn, and Sb) with relatively high concentrations as well as the presence of precious and rare elements. The concentrations of precious metals in WEEE are rather low compared with the other trace metals and thus their interactions with the precious metals are negligible. All metals are deported into different phases, *i.e.*, between metal or matte, slag and gas streams, during the smelting process.[2] The behaviors of other trace metals in copper smelting have been extensively investigated,[19–30] and further attention has been directed towards the behavior of minor elements in copper/slag/gas systems,[31–34] but only few systematic studies concerning precious metals distributions between the copper matte and slag have been published.[35, 36] With the purpose to determine the optimal conditions for the recycling of precious metals from WEEE, a significant effort is required to clarify their distribution mechanisms between matte/metal and different types of smelting and refining slags.

A. *Literature on Precious Metals Distributions in Copper Smelting*

From the point view of pyrometallurgical processing, the distributions of silver and gold have been studied more intensively during the past few decades. However, there has been limited attention to the behavior of platinum and palladium in the matte/slag system. Roghani *et al.*[37–40] conducted a series of experimental studies on the distribution behavior of Ag between matte and different slags, including FeO_x-CaO,[37] FeO_x-SiO_2-CaO,[38] FeO_x-SiO_2-MgO-based slag,[40] and SiO_2-CaO-FeO_x-MgO slags,[39] at P_{SO_2} = 0.1 to 1.0 atm and T = 1250 and 1300 °C. Consistent experimental results were reported in these studies, suggesting that the distribution coefficient of Ag ($L^{m/s}$Ag) between copper matte and slag at a given matte grade was almost constant against P_{SO_2} but increased gradually with the increase of matte grade to around 65 to 75 wt pct Cu, after which it decreased dramatically at higher matte grades. Louey *et al.*[41] determined the distribution coefficient of Ag ($L^{m/s}$Ag) between copper matte (51 to 51.5 wt pct Cu) and iron-silicate slag in MgO crucibles at 1250 °C. The $L^{m/s}$Ag was reported to be approximately 120 ± 40, which agrees well with the observations by Roghani *et al.*[37–40].

Shishin *et al.*[42] measured the distributions of Au and Ag between metallic copper/copper matte and FeO_x-SiO_2 slag at 1200 °C and P_{SO_2} = 0.25 atm. The $L^{m/s}$Ag was reported to increase when the matte grade was lower than 70 wt pct Cu, but then it started to decrease at higher matte grades. The logarithmic distribution coefficient of Au between matte and slag increased from 2.8 to 3.8 when the matte grade increased from 63 to approximately 76 wt pct Cu.

Henao *et al.*[43] investigated the distributions of Pt and Pd between copper matte and iron-silicate slag at P_{SO_2} = 0.1 atm and T = 1300 °C, in the matte grade range of 40 to 70 wt pct Cu. The $L^{m/s}$Pt and $L^{m/s}$Pd were around 1000 and were found to keep almost constant when the copper content in matte increased from 40 to 65 wt pct Cu, and then they were observed to decrease at higher matte grades.

Yamaguchi[44] studied the distributions of Au, Pt, and Pd between matte (40 to 70 wt pct Cu) and FeO_x-SiO_2-based slag in MgO crucibles at 1300 °C. CO-CO_2-SO_2 flowing gas was applied to manage the O_2, SO_2, and S_2 partial pressures of the gas atmosphere inside the experimental furnace. The distribution coefficients of Au ($L^{m/s}$Au), Pt ($L^{m/s}$Pt) and Pd ($L^{m/s}$Pd) between matte and slag were approximately stable at 1000 when copper content in matte increased from 40 to 55 wt pct Cu, and then it decreased from around 1000 to 200 with increasing matte grade.

Avarmaa *et al.*[45] reported the distributions for Au, Ag, Pt, and Pd between copper matte and silica-saturated FeO_x-SiO_2 slags within a wide matte grade interval. They conducted the experiments at 1250 °C to 1350 °C, and the gas atmosphere inside the experimental equilibrium furnace was managed by a gas mixture of CO, CO_2, SO_2, and Ar. A LA-HR ICP-MS (Laser Ablation-High Resolution Inductively Coupled Plasma-Mass Spectrometry) technique was adopted to detect the precious metals concentrations in the metallurgical slags in their study. The distribution coefficients for Au, Ag, Pt, and Pd were observed to be 1500, 150, 5000 and 3000 for 65 wt pct matte grade, respectively. They found the matte-slag distribution coefficients increased with the increase of matte grade, which are the opposite tendencies with generally observed solubilities in iron-silicate slags.[46]

Based on the above background, the impact of slag composition, including the influence of different slag modifiers, on the precious metals distributions between matte and slag has not been systematically studied. Consequently, the present work was initiated for investigating the distribution behaviors of gold, silver, platinum, and palladium between copper matte and three different slags with silica saturation (pure FeO_x-SiO_2, FeO_x-SiO_2-10 wt pct Al_2O_3, and FeO_x-SiO_2-10 wt pct Al_2O_3-10 wt pct CaO slag) at 1300 °C and P_{SO_2} = 0.1 atm, providing fundamental experimental thermodynamic information for determining the cost-effective conditions favorable for the maximum recovery of these precious metals from WEEE in the industrial copper flash smelting process.

II. EXPERIMENTAL

A. *Materials*

The experiments followed the molten slag-solid tridymite phase boundary in the FeO_x-SiO_2-Al_2O_3 and FeO_x-SiO_2-Al_2O_3-10 wt pct CaO system in equilibrium controlled gas atmosphere, shown in Figures 1 and 2.

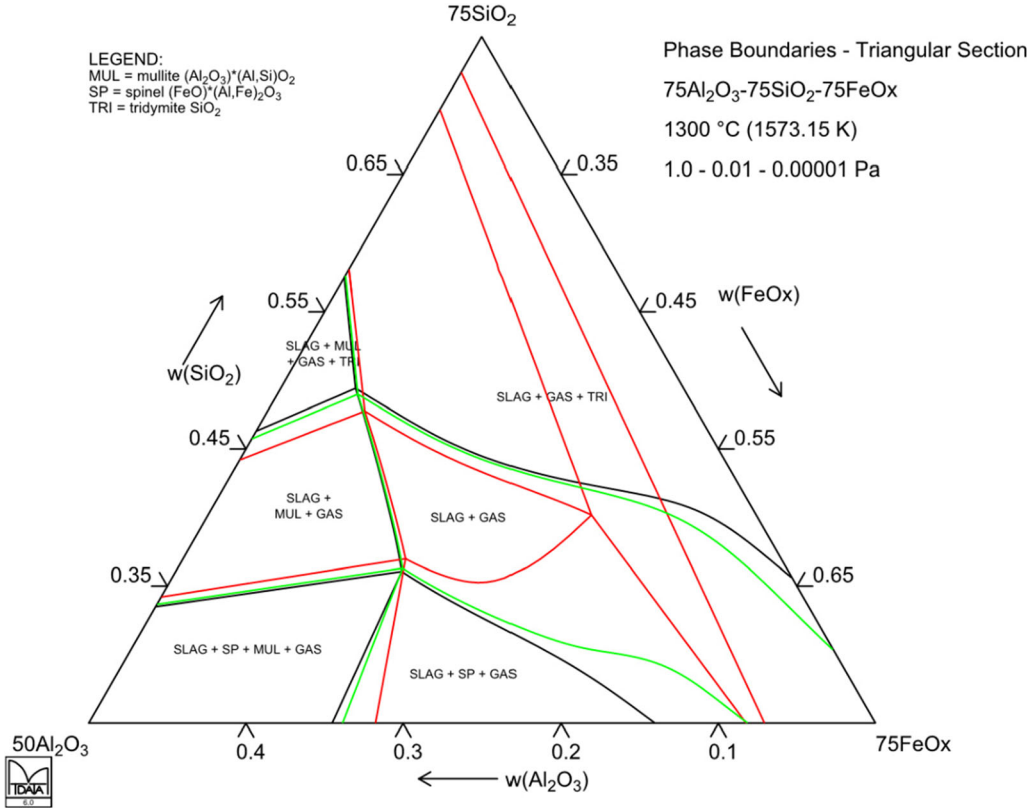

Fig. 1—The isothermal section of SiO_2-FeO_x-Al_2O_3 system at $P_{O_2} = 10^{-10}$ to 10^{-5} atm; SLAG refers to molten slag; FeO_x refers to FeO, $FeO_{1.333}$, or $FeO_{1.5}$; red line—$P_{O_2} = 10^{-5}$ atm, green line— $P_{O_2} = 10^{-7}$ atm; black line—$P_{O_2} = 10^{-10}$ atm (Color figure online).

It can be observed in Figures 1 and 2 that the increase of oxygen partial pressure has little effect on the molten slag-solid tridymite primary phase field, but the single molten slag (SLAG + GAS in Figure 1 or OX_LIQ + GAS in Figure 2) phase area increases dramatically with decreasing oxygen partial pressure. The CaO addition to the FeO_x-SiO_2-Al_2O_3 system leads to an expansion of the single molten slag phase field as well as an increase of silica solubility in the molten slag-solid tridymite phase boundary.

The slag mixtures were synthesized by high-purity oxides Fe_2O_3 (Alfa Aesar, 99.998 wt pct), SiO_2 (Alfa Aesar, 99.995 wt pct), Al_2O_3 (Sigma-Aldrich, 99.99 wt pct), and CaO (Sigma-Aldrich, 99.9 wt pct). Based on the prediction of phase boundaries which were calculated by MTDATA thermodynamic software[47,48] using MTOX database,[48] a reasonable initial slag composition was selected to be equilibrated with copper matte. The pure iron-silicate slag consisted initially of 30 wt pct SiO_2 and 70 wt pct Fe_2O_3. The exact content of each component in the starting mixture of Al_2O_3-containing slag was 47 wt pct Fe_2O_3, 43 wt pct SiO_2, and 10 wt pct Al_2O_3. For the CaO-bearing slag, the proportion of each component was weighed out to be 24 wt pct Fe_2O_3 and 56 wt pct SiO_2, 10 wt pct Al_2O_3, and 10 wt pct CaO. The copper matte was produced with an initial composition of 70 wt pct Cu_2S (99.5 wt pct)/30wt pct FeS (99.9 wt pct) for lower target matte grades and 80 wt pct Cu_2S/20 wt pct FeS for the target matte grade of 75 wt pct Cu. Each precious metal, Au (99.96 wt pct), Ag (99.95 wt pct), Pt (99.99 wt pct), and Pd (99.9 wt pct), all from Alfa Aesar, was introduced into the copper matte mixture in the form of pure metallic powders at approximately 1 wt pct concentration. Silica crucibles were used as the substrate which ensured silica saturation of the matte/slag equilibrium system and avoided additional contaminants from the crucible.

The gas atmosphere during the equilibration process was controlled by a flowing gas mixture of CO (99.99 vol pct), CO_2 (99.999 pct), SO_2 (99.99 pct), and Ar (99.999 pct), all from AGA-Linde, Finland. Nitrogen was employed to flush the working tube of the furnace after the experiments. The P_{SO_2} was fixed at 0.1 atm for all experiments. The partial pressures of O_2 and S_2 corresponding to the different gas atmosphere for varying target matte grades were calculated using MTDATA thermodynamic software with its SGTE pure substance database.[47] The calculated O_2 and S_2 partial pressures, as well as the gas flow rates used in the experiments, are listed in Table I, indicating that the matte grade increased with increasing P_{O_2} and decreasing P_{S_2}.

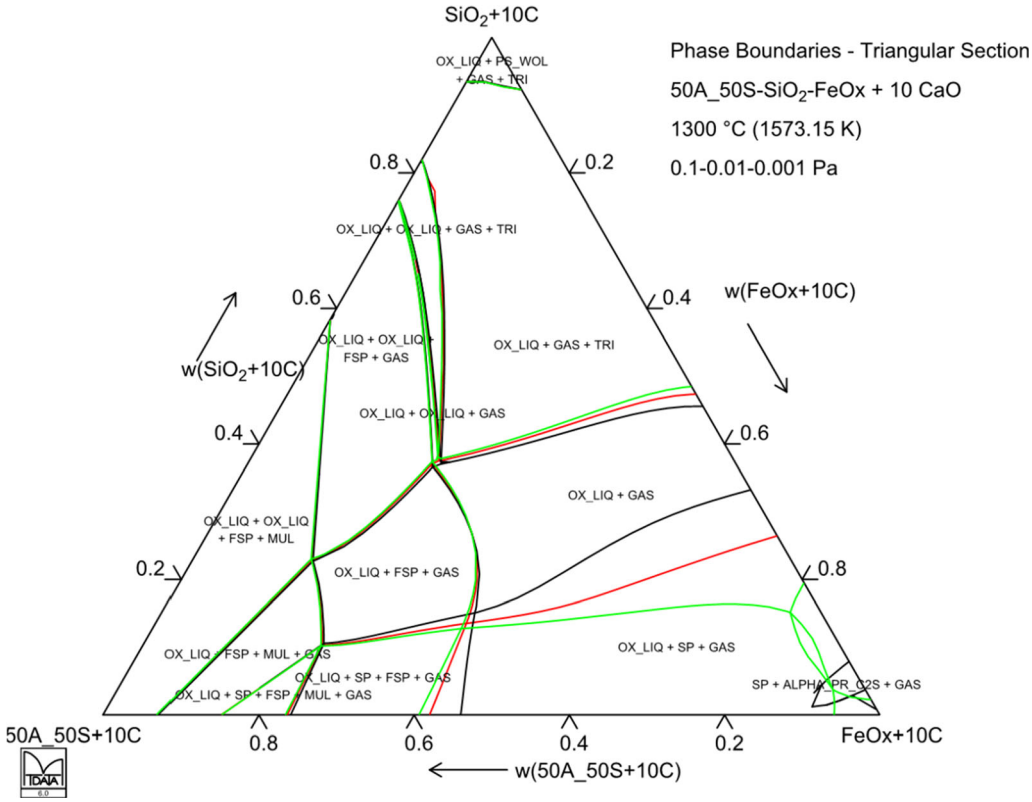

Fig. 2—The isothermal section of SiO_2-FeO_x-$AlO_{1.5}$-10 wt pct CaO system at $P_{O_2} = 10^{-8}$ to 10^{-6} atm; OX_LIQ—molten slag; 10C—10 wt pct CaO; 50A_50S—(50 wt pct $AlO_{1.5}$):(50 wt pct SiO_2); FeO_x-FeO, $FeO_{1.333}$, or $FeO_{1.5}$; TRI—tridymite; MUL—mullite; SP—spinel; FSP—feldspar; ALPHA_PR_C2S—α′ dicalcium silicate; PS_WOL—pseudo-wollastonite; green line—$P_{O_2} = 10^{-8}$ atm; red line— $P_{O_2} = 10^{-7}$ atm; black line—$P_{O_2} = 10^{-6}$ atm.

B. *Apparatus*

A vertical tube furnace (Lenton PTF 15/45/450, UK) fitted with SiC heating elements and an impervious alumina work tube was used for conducting the equilibration experiments. Eurotherm 3216 PID controllers with three-zone temperature control were used to regulate the temperature inside the furnace. An S-type Pt/90 pct Pt-10 pct Rh thermocouple (Johnson-Matthey Noble Metals, UK), calibrated beforehand at the factory, with the maximum deviation from standard ± 1.6 °C was inserted into the working tube from the top of the furnace and measured the sample temperature. The thermocouple was connected to a 2010 DMM multimeter (Keithley, USA). The thermocouple was calibrated against metallic gold and palladium at the factory. As reference points, phase transformation temperatures (solid ↔ liquid) of gold and palladium were 1064.18 ± 0.2 °C and 1553.5 ± 0.2 °C, respectively. The measurement of the cold junction was executed by a PT100 resistance thermometer (SKS Group, Finland) which was connected to a 2000 DMM multimeter (Keithley, USA). A NI LabVIEW data logging program was used to collect the temperature data during the experiments. All gas flow rates were regulated by DFC26 digital mass-flow controllers (Aalborg, USA). The schematic diagram of the equilibrium furnace and the measured temperature profile in the work tube are shown in Figure 3.

C. *Procedure*

The experiments followed the order of high-temperature isothermal equilibration in controlled flowing gas, rapid quenching in the ice-water mixture, and direct phase composition analysis by Electron Microprobe Analysis (EPMA) and LA-HR ICP-MS. Approximately 0.1 g copper matte with an equal amount of slag mixture was equilibrated in a silica crucible for each experiment. Two identical series of experiments ($5\times2\times3=30$ in total) were conducted for determining the distribution coefficients of precious metals between copper matte and three different kinds of slags. The experiments were started with weighing the right mass of slag mixture and copper matte mixture before being pressed into a pellet and placed into a silica crucible. Then the crucible was placed into a platinum basket and lifted to the cold zone of the working tube by a platinum wire from the top end of the alumina guiding tube. The bottom end of the working tube was sealed with a rubber plug. Before the equilibration, a gas mixture for getting different target matte grades was introduced into the furnace for around 30 minutes for stabilizing the atmosphere; afterward, the sample was pulled up to the hot even temperature zone for equilibration. After equilibration, the specimens were immediately dropped into the ice-water mixture for quenching.

Table I. The Calculated Gas Flow Rates and O_2 and S_2 partial Pressures Under P_{SO_2} = 0.1 atm at 1300 °C for Target Matte Grade

Target Matte Grade/wt Pct Cu	Target LogP_{O_2}/atm	Target Log P_{S_2}/atm	CO/ (mL/min)	CO_2/ (mL/min)	SO_2/ (mL/min)	Ar/ (mL/min)
55	− 8.07	− 2.28	12	15	40	300
60	− 8.00	− 2.45	12	35	40	300
65	− 7.92	− 2.63	12	55	40	300
70	− 7.79	− 2.86	9	55	40	300
75	− 7.58	− 3.27	6	55	40	300

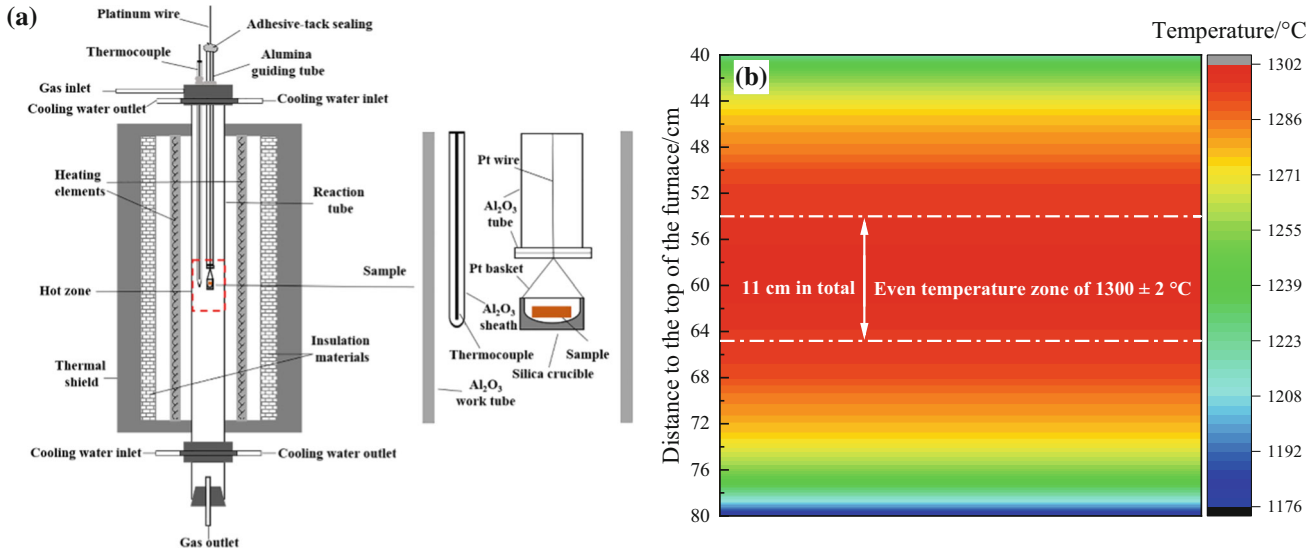

Fig. 3—The experimental equilibrium furnace (*a*) and the temperature profile (*b*) inside the work tube with a long even temperature zone of 1300 ± 2 °C.

D. *Analytical Methods*

The equilibrated samples were cut into half and embedded in epoxy resin. The cross sections were ground sequentially on 400-, 600-, 1200-, 1500-, and 4000-grit waterproof silicon carbide abrasive papers and then polished with 6-, 3-, and 1 μm-metallographic polishing cloths with diamond spray. A LEICA EM SCD050 sputtering equipment (Leica Mikrosysteme, Austria) was used for carbon-coating the polished sample surfaces. The micrographs and equilibrated phase compositions were pre-examined using a Scanning Electron Microscope (SEM; Tescan MIRA 3, Brno, Czech Republic) coupled with an UltraDry Silicon Drift energy dispersive X-ray spectrometer (EDS; Thermo Fisher Scientific, Waltham, MA, USA).

The concentrations of precious metals in matte and the main component of both matte and slag were measured with a Cameca SX100 EPMA (Cameca SAS, Genevilliers, France) fitted with five wavelength dispersive spectrometers (WDS). The analytical settings were accelerating voltage of 20 kV, beam current of 60 nA, beam diameter of 100 μm for matte and 50 to 100 μm for slag. The analysis was applied to the well-quenched, homogeneous areas without segregations. Eight point analyses were conducted for the matte and slag to improve accuracy and decrease uncertainty.

The standards used for EPMA were naturally occurring minerals, *i.e.*, quartz (Si Kα), almandine (Al Kα), hematite (Fe Kα and O Kα), galena (S Kα), diopside (Ca Kα), and pure metals Cu for Cu Kα, Pd for Pd Lα, Ag for Ag Lα, Au for Au Lα, and Pt for Pt Lα. The typical totals of the individual points were within 98 to 100.5 pct. Raw data processing before normalizing the assay was performed by a PAP-ZAF online matrix correction program.

The determination of precious metals concentrations in the slags were performed using LA-HR ICP-MS, as the precious metals concentrations in slags were too low to be analyzed with EPMA. The setup used was comprised of a Photon Machines Analyte Excite 193nm ArF laser ablation equipment (Teledyne CETAC Technologies) equipped with a Nu AttoM SC-ICP-MS (Nu Instruments Ltd, UK). Detailed information about the technique adopted in our study can be found in the reference literature.[49–51]

Table II. Detection Limits of EPMA and LA-HR ICP-MS for the Elements Investigated/ppmw

Element	O	Si	Al	Cu	Fe	Au	S	Ca	Pd	Ag	Pt
EPMA Detection Limits											
Matte	1330	100	110	320	190	650	140	110	170	170	470
Slag	1050	190	190	260	190	530	100	90	130	130	390

LA-ICP-MS Detection Limits	^{29}Si	^{197}Au	^{107}Ag	^{109}Ag	^{194}Pt	^{195}Pt	^{196}Pt	^{104}Pd
Slag	4.2386	0.0007	0.0042	0.0040	0.0015	0.0013	0.0018	0.0238

The laser spot for LA-HR ICP-MS analysis was 65 μm, and the laser energy was set to be 30.3 pct of 5.0 mJ, leading to a fluence of 2.5 J/cm^2 on the slag surface. The laser ablation analyses were performed with the following conditions: frequency of 10 Hz with 4 ns pulses, a sequence of five pre-ablation pulses, a pause of 20 seconds, gas background analysis of 20 seconds, and 400 ablation pulses. Fastscan mode was applied at low resolution ($\Delta M/M$ = 300) for collecting the Time-resolved analysis (TRA) signals. NIST 612 SRM and ^{29}Si were employed as the external and internal standards, respectively. NIST 610, USGS BCR-2G, and BHVO-2G basaltic glasses were analyzed as unknowns to monitor the equipment condition and data accuracy. The Glitter software was adopted for time-resolved analysis signal processing. Isotopes of ^{197}Au for gold, ^{104}Pd for palladium, an average of ^{107}Ag and ^{109}Ag for silver, and an average of ^{194}Pt, ^{195}Pt, and ^{196}Pt for platinum were employed to calculate the precious metals concentrations. Samples from the first series of experiments were analyzed by LA-HR ICP-MS. Eight spots were ablated from the well-quenched, homogeneous, and representative slag areas of each sample. The elemental detection limits are displayed in Table II.

III. RESULTS AND DISCUSSION

A. *Determination of Equilibration Time*

The experiments for determining the equilibration time were executed by equilibrating the pure iron-silicate slag and two different copper matte mixtures without precious metals in a silica crucible at 1300 °C and P_{O_2} = $10^{-8.07}$ and $10^{-7.58}$ atm for 2, 4, and 6 hours, respectively. Achievement of equilibration was determined based on the stabilization of the Cu, S, and O concentrations in copper matte, shown in Figure 4. The concentrations of Cu, S, and O in copper matte reached constant values after 4 hours, and therefore 4 hours was chosen as the equilibration time.

B. *Microstructures of the Copper Matte and Slag*

Typical backscattered electron (BSE) images of the equilibrium samples at 1300 °C, P_{SO_2} = 0.1 atm and $Log_{10}[P_{O_2}, atm]$ = − 7.92, for target matte grade of 65 wt pct Cu are shown in Figure 5. Matte-slag-tridymite three-phase-equilibrium was found in all samples.

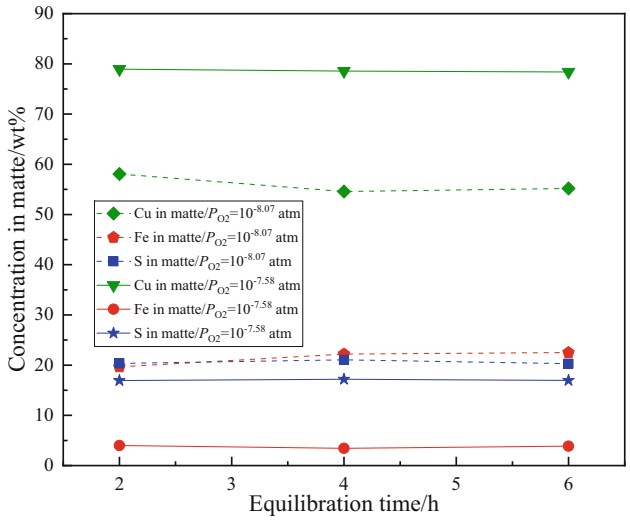

Fig. 4—The Cu, S, and O concentrations in matte *vs* equilibration time.

Tridymite, owing to the fused silica crucible and the excess of silica in the initial slag mixtures, existed as rod-like crystals in the slag and preferentially formed on the interfaces of slag and crucible. Copper-precious metals-rich textures were found in the condensed matte phase. Precious metals were segregated in the matte phase during quenching and displayed as white droplets or veins (Figure 5(b)) in the matte matrix with a typical composition measured by EDS, shown in Table III.

C. *Concentrations of Copper, Iron, and Sulfur in Matte*

Figure 6 shows the copper concentrations in matte, equilibrated with three different slags, against oxygen partial pressure, as well as the iron and sulfur concentrations against the matte grade. Results from the literature[39,52–54] were also plotted in the graphs for comparison.

It was indicated in Figure 6(a) that the copper concentration in matte increased with the increase of oxygen partial pressure, and the alumina and lime additions also caused an increase of copper concentration in matte at the same experimental conditions. There is a small discrepancy between the calculated target matte grade by MTDATA and the experimentally measured matte grade, and the discrepancy decreased with the increase of matte grade. Sukhomlinov *et al.*[53]

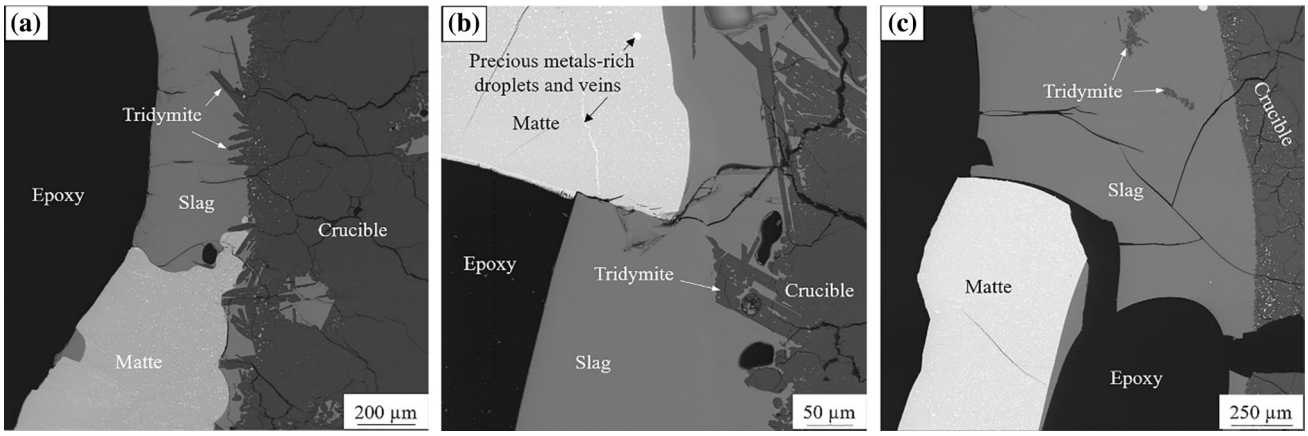

Fig. 5—BSE images of the equilibrium samples; (*a*)—63.8 wt pct Cu in matte with FeO_x-SiO_2 slag; (*b*)—65.9 wt pct Cu in matte with FeO_x-SiO_2-Al_2O_3 slag; (*c*)—68.3 wt pct Cu in matte with FeO_x-SiO_2-Al_2O_3-CaO slag.

investigated gallium, indium, tin, and tellurium distributions between copper matte and different silica-saturated iron-silicate slags, and similar results for copper concentration in matte were observed in this study, as indicated in Figure 6(a). It was reported in their study that the addition of slag modifiers Al_2O_3 and CaO into the pure acidic iron-silicate slag decreased the activity coefficient of iron oxides in silicate slags, and the consequent reduction in the activity of iron led to the decrease of iron concentration in matte.

Figures 6(b) and (c) present the iron and sulfur concentrations in matte, respectively. They have similar downward trends with increasing matte grade. The results for iron and sulfur have a good agreement with the reference studies,[39,52] but the concentrations of iron show a significant discrepancy, about 3 to 5 wt pct, with the results of Takeda's study,[54] in which the copper matte without precious metals was equilibrated with silica-saturated iron-silicate slag in MgO crucibles under a flow of SO_2-S_2-Ar gas mixture. According to the current results and the observations by Takeda,[54] it can be conservatively concluded that the copper cations in the molten matte, equilibrated with pure iron-silicate slag, were replaced by the precious metals.[52] The distributions of other major elements between matte and slag were not significantly affected by the presence of precious metals in the system.

D. *Concentrations of Precious Metals in Matte*

Figure 7 shows the concentrations of gold, silver, platinum, and palladium in matte with the experimental standard deviations, measured by EPMA. All precious metals concentrations in matte, equilibrated with all slags, seem to stay constant and have no obvious tendency of change, which indicates that the slag composition had little effect on the precious metals concentrations in matte equilibrated with the corresponding slags. The present results of precious metals concentrations in matte, equilibrated with pure iron-silicate slags, have no significant discrepancy with the study by Avarmaa *et al.*[52] It was also reported that the silver concentration in matte is highly dependent on temperature, and the increase of temperature had a reduction impact on the silver concentrations in both matte and slag.[52] This might be ascribed to the increasing volatilization of silver into the gas phase at higher temperatures.

E. *Concentrations of Copper and Precious Metals in Slags*

The slag plays an essential role in the copper flash smelting process, performing as a collector of iron oxides and gangue minerals from the raw materials, and providing options for the elimination of unwanted impurities. It is important to evaluate the concentrations of precious metals and other economic by-products retaining in the slag and minimize copper losses in slags. The copper and precious metals concentrations in slags, measured by EPMA and LA-HR ICP-MS, respectively, are displayed in Figure 8.

As shown in Figure 8(a), copper concentrations in slags increased with the increase of matte grade and oxygen partial pressure. Moreover, copper concentration in the slag was decreased by adding the basic oxides Al_2O_3 and CaO into the pure iron-silicate slag. A similar trend was observed with gold, platinum, and palladium dissolutions in slags. In most previous studies,[38–40,43,44,54,55] the MgO crucibles were used as the substrate, and the slags can be described as MgO-saturated FeO_x-SiO_2-MgO[38,40,43,44,54,55] or FeO_x-SiO_2-MgO-CaO[38,39] slags. The copper concentrations in the FeO_x-SiO_2-MgO[38,54] slags at MgO saturation are slightly on the lower side than the results in the SiO_2-saturated FeO_x-SiO_2-Al_2O_3 slags in this study, except for the results of the literature,[40,43,44,55] which are slightly higher than those in the FeO_x-SiO_2-Al_2O_3 slags in the present work. The copper concentrations in the MgO-saturated FeO_x-SiO_2-MgO-CaO[38,39] slags are approximately 0.2 to 0.3 wt pct lower than those in the SiO_2-saturated FeO_x-SiO_2-CaO-Al_2O_3 slags investigated in the present research. The copper concentrations in SiO_2-saturated pure FeO_x-SiO_2 slags in the present study fit well with the results by Avarmaa *et al.*,[52] and the reduction effects of basic oxides Al_2O_3 and CaO in

Table III. Typical Composition of Copper-Precious Metals-Rich Droplets in the Matte Formed During the Quenching

Element	O	Si	S	Fe	Cu	Pd	Ag	Pt	Au
Content	0.2(3) ± 0.16	0.0(7) ± 0.01	0.5(9) ± 0.03	2.0(7) ± 0.05	32.6(3) ± 0.05	10.7(4)± 0.14	0.5(0) ± 0.09	32.6(2) ± 1.28	20.5(5) ± 1.16

SiO_2-saturated iron-silicate slag on the copper concentration in slags were also observed by Sukhomlinov *et al.*[53]

Typically, the viscosity of the iron-silicate slag with a high SiO_2 concentration is higher than that of the corresponding slag in which the SiO_2 concentration has been decreased by basic oxide additions such as Al_2O_3, MgO, and CaO. Kim and Sohn[56] investigated the effects of Al_2O_3, MgO, and CaO additions in iron-silicate slag with silica saturation on the minor element and copper distributions in the metallic copper and iron-silicate slag system, and similar results to the present study were obtained. The high viscosity of the silica-rich slag is mainly attributed to the existence of polymeric silicate anions which formed a stable three-dimensional network, but the network can be decomposed by the addition of basic oxides,[57,58] thus leading to the decrease of copper, gold, platinum, and palladium mechanically entrained losses in slags. However, in the present study, we focused on the chemically dissolved precious metals measured in micrometric volumes of slags, which cannot be affected by the increase of viscosity. It was also reported by Mackey *et al.*[58] that Al_2O_3, MgO, and CaO perform in respective order as increasingly basic oxides in iron-silicate slags, replacing copper cations while occupying sites within the silica structure, thereby decreasing the chemically dissolved copper in slags. This view is supported by comparing the copper concentrations in slags from the literature[38,39,54] and the present study.

The gold concentrations in all slags decreased throughout the matte grade range investigated, but the slope was less steep with alumina and lime additions. Shishin *et al.*[42] investigated the behavior of gold between pure metallic gold and FeO_x-SiO_2 slag in equilibrium with tridymite, reporting that the solubility of gold in the slag was quite low, ranging approximately from 1.1 to 2.1 ppm, which is within the range of the observations in the present study. It was reported by Swinbourne *et al.*[59] that the solubility of gold in FeO_x-SiO_2 and CaO-FeO_x slags increased along with the increase of oxygen partial pressure, and the gold was indicated to exist in the form of Au^+ ions in the molten slags. The trend is opposite with the present results but fit well with the observations in the study by Han *et al.*,[60] in which the behavior of gold in magnesia-saturated CaO-SiO_2-Al_2O_3-MgO slags was investigated, reporting that the gold dissolved into the CaO-SiO_2-Al_2O_3-MgO slags in the form of AuO^- or AuO_2^{3-}, and the solubility of gold in slags can be increased by increasing the oxygen partial pressure as well as increasing the activity of CaO.

The platinum and palladium concentrations in pure iron-silicate slags and alumina-containing slags have downward trends, as reported by Avarmaa *et al.*,[45] but they remain nearly constant in the alumina + lime-containing slags. Figures 8(b), (d), and (e) indicate that the chemical dissolutions of gold, platinum, and palladium in slags were inhibited by the alumina and lime addition. Yamaguchi[55] investigated the behavior of palladium in the Pd-Cu alloy/slag system within the same partial pressure range as the present study, and the measured

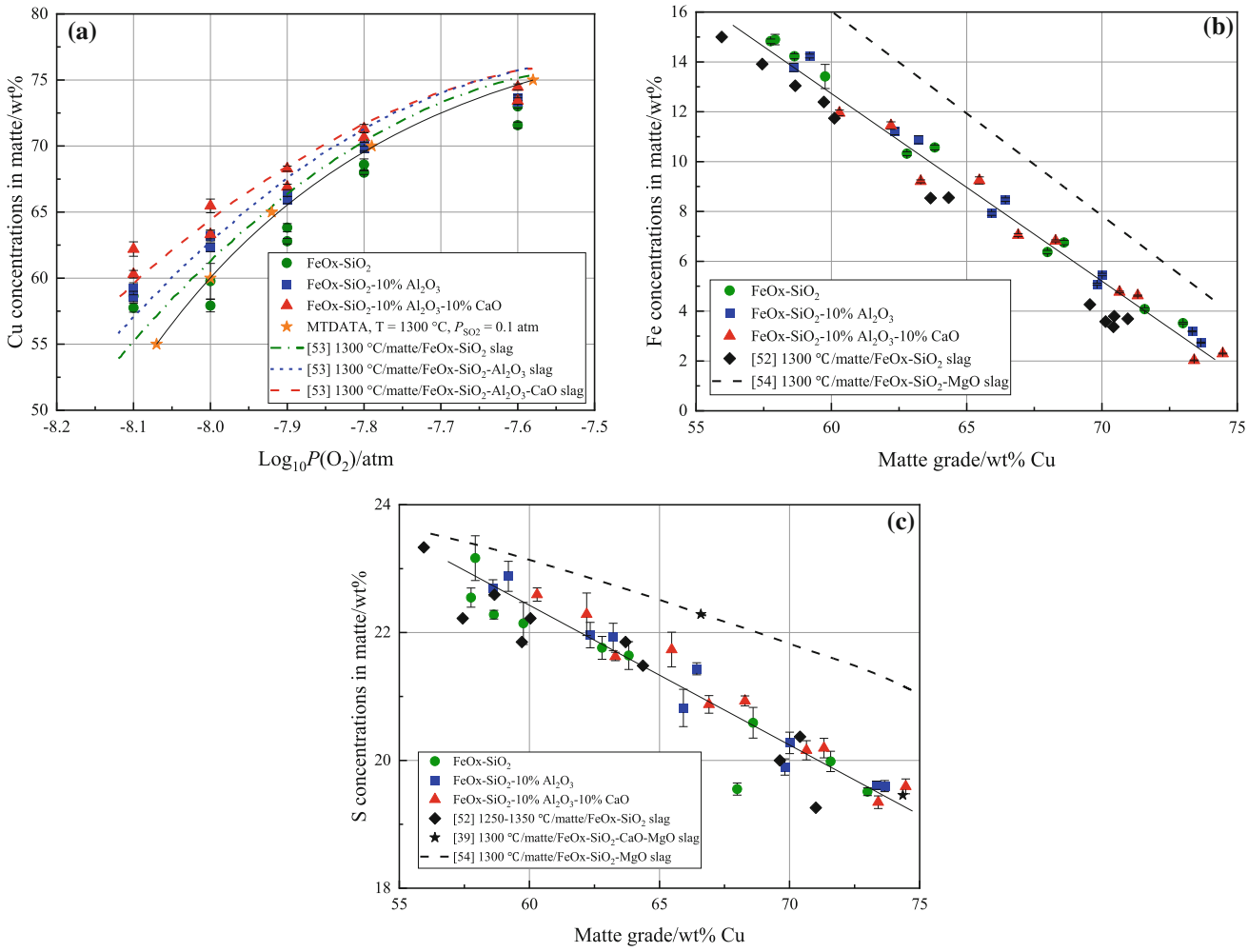

Fig. 6—The concentrations of copper (*a*), iron (*b*), and sulfur (*c*) in matte equilibrated with different slags at 0.1 atm SO_2 *vs* oxygen partial pressure or matte grade at 1300 °C.

palladium concentrations in slag were from 10 to 17 ppm which are slightly higher than the results in the present study.

As for the silver concentration in the pure iron-silicate slag, it kept approximately constant when the copper content in matte increased from 58 to around 65 wt pct Cu, after which it decreased dramatically at higher matte grades. The results for silver in pure iron-silicate slags are within the range of the observations by Avarmaa *et al.*[45] Silver concentrations in alumina-containing slags and lime-containing slags were lower than those in pure iron-silicate slag when the matte grade varied from 55 to approximately 70 wt pct Cu and tended to increase at higher matte grades. The concentration of silver in all silica-saturated slags investigated in this study was markedly higher than that of gold and platinum group metals. The increasing trends of alumina-containing and lime-containing slags were also found in the literature [61], in which the behavior of silver was investigated between molten copper and FeO_x-SiO_2-Al_2O_3 slags at 1300 °C. It was reported by Avarmaa *et al.*[45] that the silver concentration in slags decreased with increasing temperature. Xiong *et al.*[62] and Sheets *et al.*[63] reported that silver can have interactions with Al_2O_3 under certain conditions forming $AgAlO_2$, which can explain the increase of chemical dissolutions of silver in slags.

F. *Distributions of Precious Metals Between Copper Matte and Slag*

The distribution coefficients between copper matte and slag are fundamental parameters for determining how effectively the precious metals can be recycled through the copper matte smelting process, by utilizing the copper matte as a collector for precious metals. The distribution coefficients of precious metals between copper matte and slag, $L^{m/s}(Me)$, were calculated using the following equation [1] from the experimental data:

$$\mathrm{Log}_{10}L^{m/s}(\mathrm{Me}) = \mathrm{Log}_{10}([\text{wt pct Me}]/(\text{wt pct Me})), \quad [1]$$

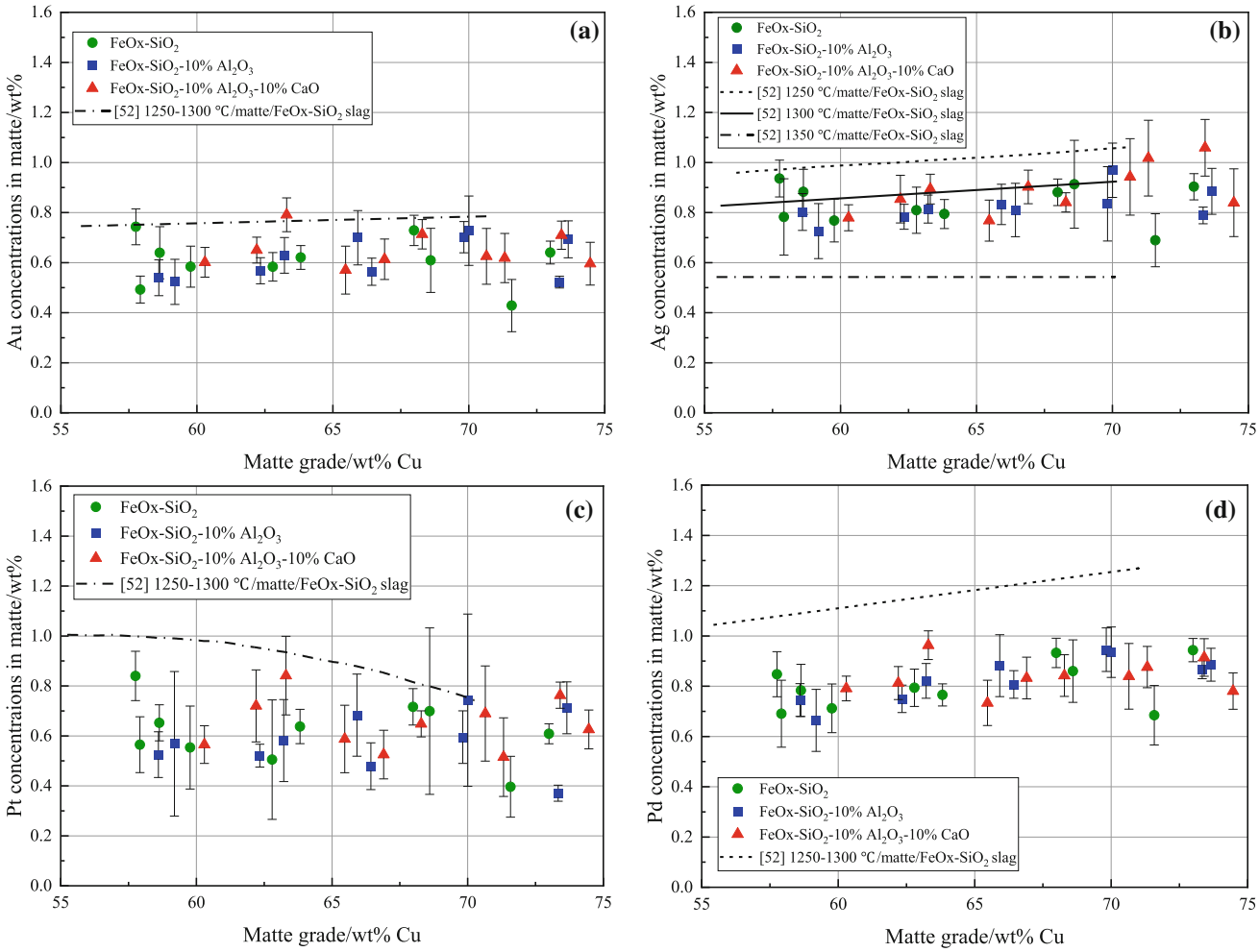

Fig. 7—Precious metals concentrations in matte equilibrated with different slags at 0.1 atm SO_2, 1300 °C: (*a*) gold; (*b*) silver; (*c*) platinum; (d) palladium.

where the brackets [wt pct Me] and (wt pct Me) refer to the measured average precious metals concentrations in matte and slag, respectively. The distribution results for each precious metal investigated in this study are shown in Figure 9.

The distribution coefficients between copper matte and slag for all precious metals were significantly affected by the slag composition. The slag modifiers Al_2O_3 and CaO had different impacts on the distribution coefficients of the precious metals investigated. The distribution coefficients of gold, $L^{m/s}$Au, increased along with the increase of matte grade, which agrees well with the most recent study,[45] although an opposite trend was reported by Henao *et al.*[43] and Yamaguchi.[44] The alumina and lime additions improved the distribution coefficients of gold by varying degrees. Therefore, it can be concluded that the recoveries of precious metals through the copper flash smelting process can be improved by increasing the matte grade as well as adding basic oxides into the iron-silicate slags.

The trend line of the distribution coefficient for silver, $L^{m/s}$Ag, between copper matte and pure FeO_x-SiO_2 slag indicates its preference to be deported into the copper matte with the increase of matte grade. This observation is very close to that reported by Avarmaa *et al.*[45] However, silver has an opposite downward trend with the increase of matte grade in the matte/alumina-containing slag and matte/alumina + lime-containing slag systems. The logarithmic distribution coefficient between matte and alumina + lime-containing slag was about 0.2 logarithmic units higher than that between matte and pure iron-silicate/alumina-containing slag throughout the matte grade range investigated. Thus, lime improved the recovery of silver in matte, whereas alumina did not have a clear influence on the $L^{m/s}$(Ag) when compared to pure iron-silicate slag. Similar observations were made by Avarmaa[64] for the copper-slag system. In the studies between copper matte and FeO_x-CaO,[37] FeO_x-SiO_2-MgO,[40] and FeO_x-SiO_2-MgO-CaO[39] slag, the distribution coefficient of

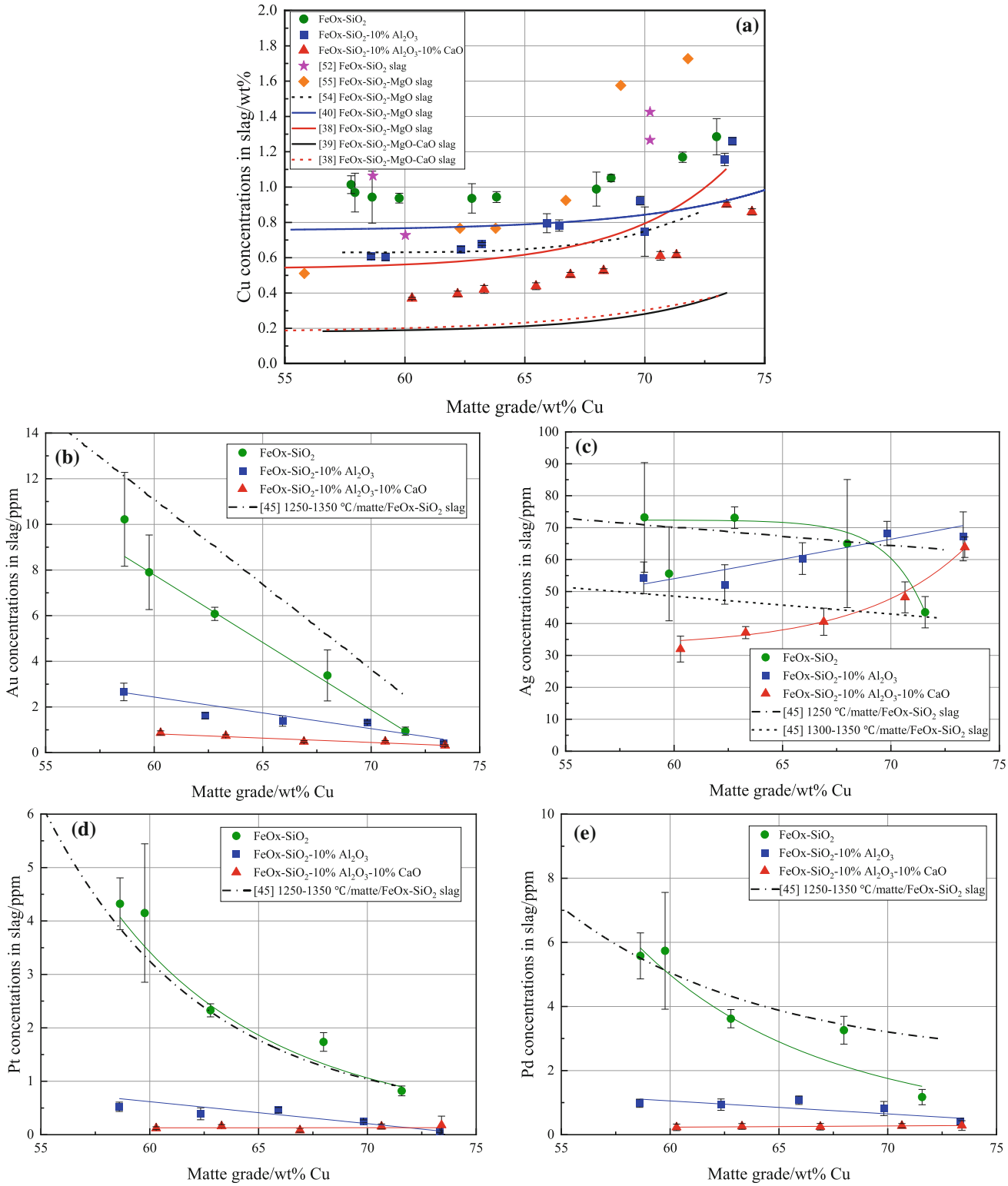

Fig. 8—Copper and precious metals concentrations in silica-saturated slags against copper matte grade: (*a*) copper; (*b*) gold; (*c*) silver; (*d*) platinum; (*e*) palladium.

silver increased gradually along with the matte grade up to around 65 to -75 wt pct Cu, after which it decreased abruptly at higher matte grades.

The present results are slightly lower than the previous observations[39,40] studied at MgO saturation. The distribution coefficients of silver were lower than those of the other three precious metals because its

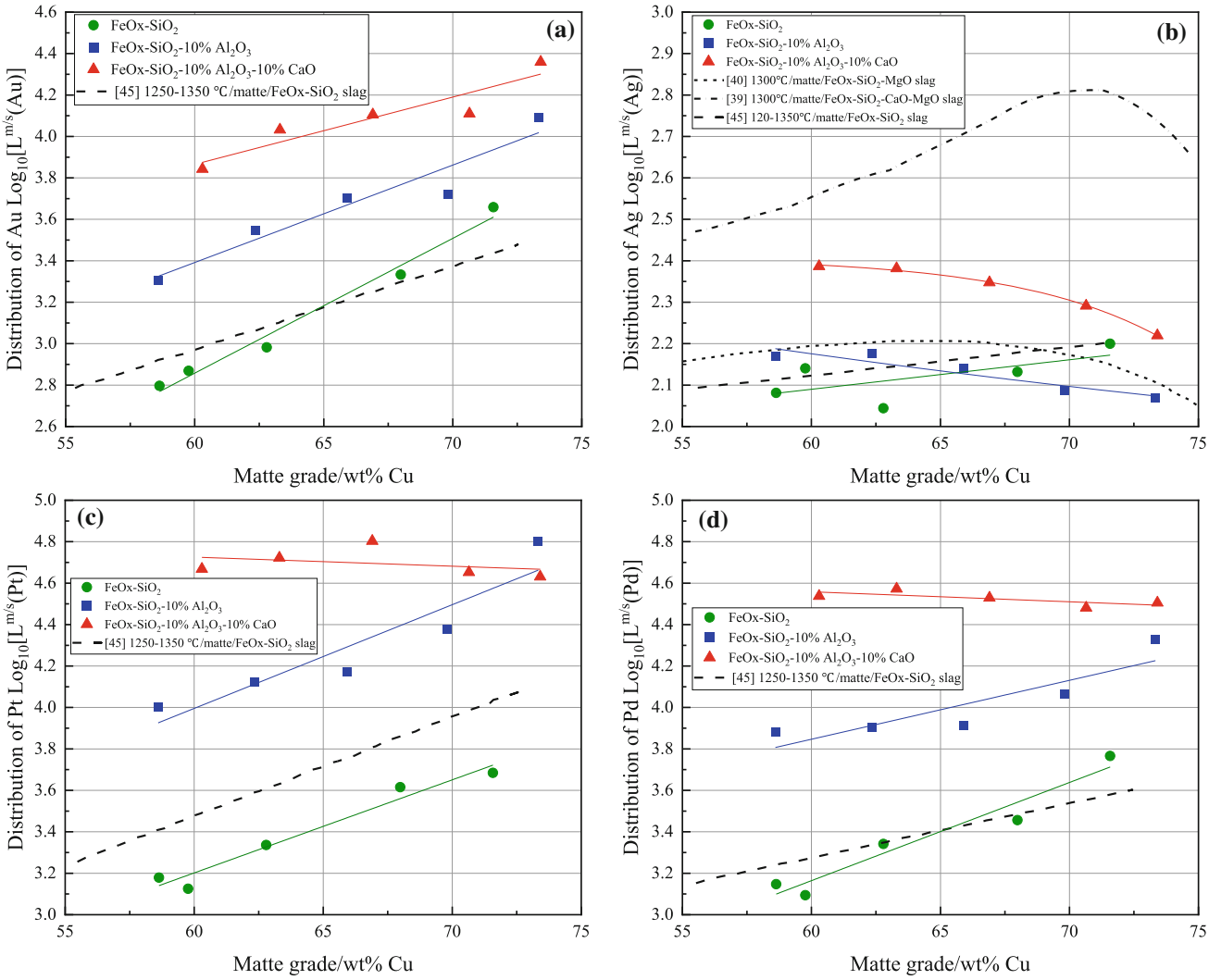

Fig. 9—Logarithmic distribution coefficients of gold (*a*), silver (*b*), platinum (*c*), and palladium (*d*) between copper matte and slag *vs* matte grade.

affinity for oxygen is higher than that of other precious metals investigated in this study, resulting in more silver being oxidized into the molten slag phase. Based on the present results and the previous studies,[45,52] it can be concluded that a lower matte grade and lower temperature are preferable for the deporting of silver into the matte phase. Kashima *et al.*[65] proposed the metallic dissolution of silver in the slag. Takeda *et al.*[66] suggested that silver existed as metallic silver in slag in the lower oxygen partial pressure range, but dissolved into the slag as monovalent oxide of $AgO_{0.5}$ at high oxygen partial pressure conditions. Roghani *et al.*[39] reported that silver dissolved in the slag as $AgS_{0.5}$ when the matte grade was less than 70 wt pct Cu and mainly existed as $AgO_{0.5}$ at higher matte grades. These studies mentioned above provide some guidance for investigating the existing form of precious metals in the copper matte/slag equilibrium system.

The experimental distribution coefficients for platinum and palladium in the matte/iron-silicate slag system displayed a similar increasing trend with the increase of matte grade with the reference study,[45] increasing from the initial logarithmic value of 3.1 at the low matte grade to around 3.8 at the higher matte grade side. As for the distribution coefficients of platinum and palladium in the matte/alumina-containing slag system, the deportment to matte for both platinum and palladium increased gradually with increasing matte grade, but the increasing trend for platinum was more vigorous. In the matte/alumina + lime-containing slag system, the logarithmic distribution coefficients $Log_{10}[L^{m/s}Pt]$ and $Log_{10}[L^{m/s}Pd]$ were steady and fluctuated around the logarithmic value of 4.7 and 4.5, respectively. In a study by Yamaguchi,[55] results opposite to this study were obtained, concluding that the logarithmic distribution coefficients of platinum and palladium between copper matte and slag at MgO saturation kept almost constant with $Log_{10}L^{m/s}(Me) = 3$ when the matte grade varied from 40 to 65 wt pct Cu. However, the distribution coefficients decreased when the matte grade was higher than 65 wt pct Cu. Yamaguchi[55] measured the platinum and palladium concentrations in matte and slag by a wet chemical analysis after physically separating the slag and matte.

Most likely an incomplete separation of slag and matte, as well as the physical inclusion of tiny matte droplets in the slag caused the decreased distribution coefficients measured in that study.

IV. CONCLUSIONS

The copper flash smelting process is an effective and high potential technology for treating WEEE due to the advantages of high feeding rate, increased production output, low energy consumption, and the high-concentration SO_2 by-product for making sulfuric acid. However, there is limited information about the precious metals distributions between copper matte and FeO_x-SiO_2-based slag with silica saturation. As a contribution to the understanding of recycling precious metals from WEEE through the copper flash smelting technology, the distribution coefficients of precious metals Au, Ag, Pt, and Pd between copper matte and three different silica-saturated FeO_x-SiO_2-based slags were determined at 1300 °C in controlled CO-CO_2-SO_2-Ar gas atmospheres by high-temperature isothermal equilibration technique. EPMA and LA-HR ICP-MS techniques were used for measuring the precious metals concentrations in matte and slag with high sensitivity. This is the first report of the LA-HR ICP-MS method being applied to measure the concentrations of selected precious metals in Al_2O_3-containing slags and Al_2O_3 + CaO-containing slags in the copper matte/slag system.

All precious metals were found to deport strongly into the matte phase rather than into the slag, indicating that copper matte performs as an excellent collector for them. The addition of basic oxides Al_2O_3 and CaO into iron-silicate slags decreased the concentrations of Au, Pt, and Pd in slags, ranging from 0 to 12 ppm, but favored the distributions of these precious metals to the matte phase. The recovery of Ag in matte was improved by CaO addition, whereas Al_2O_3 did not have a clear influence on the $L^{m/s}$(Ag). The distributions of Au, Pt, and Pd into matte were found to increase with increasing matte grade. However, the distributions of Ag into the Al_2O_3-containing slags and Al_2O_3 + CaO-containing slags were found to increase in the range of 30 to 70 ppm as the matte grade increased. The experimentally measured distribution coefficients $L^{m/s}$(Me) followed the order of Pt > Pd > Au > Ag.

As the present results on ternary iron-silicate slags fit well with earlier observations in the literature,[45] we are confident that the current data on Al_2O_3- and CaO-bearing slags are also reliable.

ACKNOWLEDGMENTS

Open access funding provided by Aalto University. This work was partly financially supported by the Aalto University School of Chemical Engineering and the Business Finland financed SYMMET project [Grant Number 3891/31/2018], and utilized the Academy of Finland's RawMatTERS Finland Infrastructure (RAMI) based at Aalto University, GTK Espoo and VTT Espoo. The contribution of Mr. Lassi Pakkanen from Geological Survey of Finland (GTK) is specially appreciated for conducting the EPMA analyses. Min Chen acknowledges the China Scholarship Council [Grant Number 201806370217] for supporting his study at Aalto University.

CONFLICT OF INTEREST

None.

OPEN ACCESS

REFERENCES

1. J. Cui and L. Zhang: *J. Hazard. Mater.*, 2008, vol. 158 (2–3), pp. 228–56.
2. M.A.H. Shuva, M.A. Rhamdhani, G.A. Brooks, S. Masood, and M.A. Reuter: *J. Cleaner Prod.*, 2016, vol. 131, pp. 795–809.
3. M.A. Reuter and I.V. Kojo: *World Metall.-Erzmet.*, 2014, vol. 67(1), pp. 5–12.
4. J. Shi, M. Chen, I. Santoso, L. Sun, M. Jiang, P. Taskinen, and A. Jokilaakso: *Ceram. Int.*, 2020, vol. 46 (2), pp. 1545–50.
5. J. Cui and E. Forssberg: *J. Hazard. Mater.*, 2003, vol. 99 (3), pp. 243–63.
6. O.A. Ogunseitan, J.M. Schoenung, J.D.M. Saphores, and A.A. Shapiro: *Science*, 2009, vol. 326 (5953), pp. 670–71.
7. T. Yang, P. Zhu, W. Liu, L. Chen, and D. Zhang: *Waste Manage.*, 2017, vol. 68, pp. 449–57.
8. L. Zhang and Z. Xu: *J. Cleaner Prod.*, 2016, vol. 127, pp. 19–36.
9. A. Cesaro, A. Marra, K. Kuchta, V. Belgıorno, and E.D. Van Hullebusch: *Global NEST J.*, 2018, vol. 20, pp. 743–50.
10. A. Akcil, C. Erust, C.S. Gahan, M. Ozgun, M. Sahin, and A. Tuncuk: *Waste Manage.*, 2015, vol. 45, pp. 258–71.
11. K. Huang, J. Guo, and Z. Xu: *J. Hazard. Mater.*, 2009, vol. 164 (2–3), pp. 399–08.
12. P. Hense, K. Reh, M. Franke, J. Aigner, A. Hornung, and A. Contin: *Environ. Eng. Manage. J.*, 2015, vol. 14 (7), pp. 1637–47.
13. O. Tsydenova and M. Bengtsson: *Waste Manage.*, 2011, vol. 31 (1), pp. 45–58.
14. J. Brusselaers, F.E. Mark, and L. Tange: Technical Report, Plastics Europe, Brüssels, Belgium, 2006. Accessed at https://www.isasmelt.com/en/download/TechnicalPapersIsasmelt/Using_metal-rich_WEEE_plastics_as_feed.pdf.
15. C. Hagelüken: *Acta Metall. Slovaca*, 2006, vol. 12, pp. 111–20.
16. C. Hagelüken: *World Metall.-Erzmet.*, 2006, vol. 59(3), pp. 152–61.

17. A. Lennartsson, F. Engström, C. Samuelsson, B. Björkman, and J. Pettersson: *J. Sustain. Metall.*, 2018, vol. 4 (2), pp. 222–32.
18. J. Sulanto: in *VTT Symposium on Non-Waste Technology*, Espoo, Finland, 1988, pp. 20–23.
19. A. Dańczak, L. Klemettinen, M. Kurhila, P. Taskinen, D. Lindberg, and A. Jokilaakso: *Batteries*, 2020, vol. 6 (1), pp. 16. https://doi.org/10.3390/batteries6010016.
20. T. Tirronen, D. Sukhomlinov, H. O'Brien, P. Taskinen, and M. Lundström: *J. Cleaner Prod.*, 2017, vol. 168, pp. 399–409.
21. D. Sukhomlinov, K. Avarmaa, O. Virtanen, P. Taskinen, and A. Jokilaakso: *Miner. Process. Extr. Metall. Rev.*, 2020, vol. 41 (3), pp. 171–77.
22. L. Klemettinen, K. Avarmaa, H. O'Brien, P. Taskinen, and A. Jokilaakso: *Minerals*, 2019, vol. 9 (1), pp. 39–54.
23. K. Avarmaa, L. Klemettinen, H. O'Brien, P. Taskinen, and A. Jokilaakso: *Minerals*, 2019, vol. 9 (6), pp. 367–79.
24. D. Sukhomlinov and P. Taskinen: in *Proceedings of the European Metallurgical Conference (EMC)*, 3, GDMB, Clausthal-Zellerfeld, 2017, pp. 1029–38.
25. K. Avarmaa and P. Taskinen: in *Proceedings of Extraction 2018*, Ottawa, Springer, Cham, 2018, pp. 1061–71.
26. Q. Wang, X. Guo, Q. Tian, T. Jiang, M. Chen, and B. Zhao: *Metals*, 2017, vol. 7 (11), pp. 502–12.
27. T. Hidayat, J. Chen, P.C. Hayes, and E. Jak: *Metall. Mater. Trans. B*, 2019, vol. 50B, pp. 229–41.
28. A. Anindya, D.R. Swinbourne, M.A. Reuter, and R.W. Matusewic: *Miner. Process. Extr. Metall.*, 2013, vol. 122 (3), pp. 165–73.
29. G.H. Kaiura, K. Watanabe, and A. Yazawa: *Can. Metall. Q.*, 1980, vol. 19 (2), pp. 191–200.
30. M. Nagamori, P.J. Mackey, and P. Tarassoff: *Metall. Trans. B*, 1975, vol. 6 (2), pp. 295–301.
31. K. Avarmaa, S. Yliaho, and P. Taskinen: *Waste Manage.*, 2018, vol. 71, pp. 400–10.
32. K. Avarmaa, L. Klemettinen, H. O'Brien, and P. Taskinen: *Miner. Eng.*, 2019, vol. 133, pp. 95–102.
33. L. Klemettinen, K. Avarmaa, and P. Taskinen: *J. Sustain. Metall.*, 2017, vol. 3 (4), pp. 772–81.
34. D. Sukhomlinov, K. Avarmaa, O. Virtanen, P. Taskinen, and A. Jokilaakso: *Miner. Process. Extr. Metall. Rev.*, 2020, vol. 41 (1), pp. 32–40.
35. P. Dordević, N. Mitevska, I. Mihajlović, D. Nikolić, D. Manasijević, and Z. Zivković: *J. Min. Metall. Sect. B*, 2012, vol. 48(1), pp. 143-51.
36. E. Jak, D. Hidayat, V. Prostakova, D. Shishin, M. Shevchenko, and P.C. Hayes: in *Proc. European Metall. Conf. EMC 2019*, vol 2, 23–26 June 2019, Dusseldorf, Germany, GDMB, Clausthal-Zellerfed, 2019, pp. 587-604.
37. G. Roghani, J.C. Font, M. Hino, and K. Itagaki: *Mater. Trans. JIM*, 1996, vol. 37 (10), pp. 1574-79.
38. G. Roghani, M. Hino and K. Itagaki: in *Proc. 5th Int. Conf. on Molten Slags, Fluxes and Salts*. Iron & Steel Society, Warrendale, PA, 1997, pp. 693–703.
39. G. Roghani, M. Hino, and K. Itagaki: *Mater. Trans. JIM*, 1997, vol. 38(8), pp. 707–13.
40. G. Roghani, Y. Takeda, and K. Itagaki: *Metall. Mater. Trans. B*, 2000, vol. 31B, pp. 705–12.
41. R. Louey, D.R. Swinbourne, and T. Lehner: in *AusIMM Proceedings*, The Australian Institute of Mining and Metallurgy, 1999, vol. 304, pp. 31–36.
42. D. Shishin, T. Hidayat, J. Chen, P.C. Hayes, and E. Jak: *J. Sustain. Metall.*, 2019, vol. 5 (2), pp. 240–49.
43. H.M. Henao, K. Yamaguchi, and S. Ueda: in *Proc. Sohn International Symposium*, F. Kongoli and R. Reddy, eds., TMS, Warrendale, PA, 2006, vol. 1, pp. 723–29.
44. K. Yamaguchi: in *Proc. Copper 2010*, GDMB, Clausthal-Zellerfeld, Germany, 2010, vol. 3, pp. 1287–95.
45. K. Avarmaa, H. O'Brien, H. Johto, and P. Taskinen: *J. Sustain. Metall.*, 2015, vol. 1 (3), pp. 216–28.
46. A. Borisov and H. Palme: *Am. Mineral.*, 2000, vol. 85, pp. 1665–73.
47. R.H. Davies, A.T. Dinsdale, J.A. Gisby, J.A.J. Robinson, and A.M. Martin: *Calphad*, 2002, vol. 26 (2), pp. 229–71.
48. J. Gisby, P. Taskinen, J. Pihlasalo, Z. Li, M. Tyrer, J. Pearce, K. Avarmaa, P. Björklund, H. Davies, M. Korpi, S. Martin, L. Pesonen, and J. Robinson: *Metall. Mater. Trans. B*, 2017, vol. 48B (1), pp. 91–98.
49. J. Lin, Y. Liu, Y. Yang, and Z. Hu: *Solid Earth Sci.*, 2016, vol. 1 (1), pp. 5–27.
50. D. Sukhomlinov, L. Klemettinen, K. Avarmaa, H. O'Brien, P. Taskinen, and A. Jokilaakso: *Metall. Mater. Trans. B*, 2019, vol. 50B, pp. 1752–65.
51. P. Sylvester: *Laser ablation-ICP-MS in the earth sciences: current practices and outstanding issues*, Mineralogical Association of Canada, Québec, Canada, 2008, vol. 40, pp. 1–348.
52. K. Avarmaa, H. Johto, and P. Taskinen: *Metall. Mater. Trans. B*, 2016, vol. 47B, pp. 244–55.
53. D. Sukhomlinov, L. Klemettinen, H. O'Brien, P. Taskinen, and A. Jokilaakso: *Metall. Mater. Trans. B*, 2019, vol. 50B, pp. 2723–32.
54. Y. Takeda: in *Proc. '97 Conf. Molten Slags, Fluxes and Salts*, Sydney, Iron & Steel Society, Warrendale, PA, 1997, pp. 329–39.
55. K. Yamaguchi: in *Proc. Extraction 2018*, Ottawa, Springer, Cham, 2018, pp. 797–804.
56. H.G. Kim and H.Y. Sohn: *Metall. Mater. Trans. B*, 1998, vol. 29B, pp. 583–90.
57. B. Keyworth: in *Proc. Precious Metals 1982*, California, Pergamon Press, 1983, pp. 509-37.
58. P.J. Mackey: *Can. Metall. Q.*, 1982, vol. 21 (3), pp. 221–60.
59. D.R. Swinbourne, S. Yan, and S. Salim: *Miner. Process. Extr. Metall.*, 2005, vol. 114 (1), pp. C23–C29.
60. Y.S. Han, D.R. Swinbourne, and J.H. Park: *Metall. Mater. Trans. B*, 2015, vol. 46B, pp. 2449–57.
61. K. Avarmaa, H. O'Brien, and P. Taskinen: in *Proceedings of the 10th International Conference on Molten Slags, Fluxes and Salts 2016*, R.G. Reddy, P. Chaubal, and P.C. Pistorius, and U. Pal, eds., Advances in Molten Slags, Fluxes, and Salts, 2016, Springer, Cham. https://doi.org/10.1007/978-3-319-48769-4_20.
62. D. Xiong, X. Zeng, W. Zhang, H. Wang, X. Zhao, W. Chen, and Y.B. Cheng: *Inorg. Chem.*, 2014, vol. 53 (8), pp. 4106–16.
63. W. Sheets, E.S. Stampler, M.I. Bertoni, M. Sasaki, T.J. Marks, T.O. Mason, and K.R. Poppelmeier: *Inorg. Chem.*, 2008, vol. 47 (7), pp. 2696–2705.
64. K. Avarmaa: *PhD thesis*, Aalto University, 2019. Accessed at https://aalto.finna.fi/Record/aaltodoc.123456789_39995.
65. M. Kashima, M. Eguchi, and A. Yazawa: *Trans. Jpn. Inst. Met.*, 1978, vol. 19 (3), pp. 152–58.
66. Y. Takeda, S. Ishiwata, and A. Yazawa: *Trans. Jpn. Inst. Met.*, 1983, vol. 24 (7), pp. 518–28.